Coordination Properties of the Oxime Analogue of Glycine to Cu(II)

I. Georgieva,[†] N. Trendafilova,*,[†] L. Rodríguez-Santiago,[‡] and M. Sodupe*,[‡]

Institute of General and Inorganic Chemistry, Bulgarian Academy of Sciences, 1113 Sofia, Bulgaria, and Departament de Quimica, Unitat de Quimica Fisica, Universitat Autònoma de Barcelona, 08193 Bellaterra, Barcelona, Spain

Received: February 4, 2005; In Final Form: April 26, 2005

The coordination of Cu^{2+} by glyoxilic acid oxime (gao) − the oxime analogue of glycine amino acid − and its deprotonated (gao^- and gao^{2-}) species has been studied with different density functional methods. Single-point calculations have also been carried out at the single- and double- (triple) excitation coupled-cluster (CCSD(T)) level of theory. The isomers studied involve coordination of Cu^{2+} to electron-rich sites (O,N) of neutral, anionic, and dianionic gao species in different conformations. In contrast to Cu^{2+}−glycine, for which the ground-state structure is bidentate with the CO_2^- terminus of zwitterionic glycine, for Cu^{2+}−gao the most stable isomer shows monodentate binding of Cu^{2+} with the carbonylic oxygen of the neutral form. The most stable complexes of Cu^{2+} interacting with deprotonated gao species (gao^- and gao^{2-}) also take place through the carboxylic oxygens but in a bidentate manner. The results with different functionals show that, for these open shell (Cu^{2+}−L) systems, the relative stability of complexes with different coordination environments (and so, different spin distribution) can be quite sensitive to the amount of "Hartree−Fock" exchange included in the functional. Among all the functionals tested in this work, the BHandHLYP is the one that better compares to CCSD(T) results.

I. Introduction

The growing interest and extensive studies both in solution[1−5] and in the solid state[5−13] of 2-(hydroxyimino)carboxylic acids (2-hica), R−C(=NOH)COOH, (oxime analogues of amino acids) are due to their original coordination properties to metal ions. These oxime derivatives have applications in several fields: in analytical chemistry and metallurgy as very effective complexing agents,[14] in metal oxide ceramics as low-temperature precursors,[15] in organometallic reactions as suitable matrixes,[16] in molecular magnetism for design and synthesis of polynuclear assemblies,[17] and in biochemistry.[18]

By versatile conditions (pH, solvent, and temperature), the neutral, anionic, and dianionic species of 2-(hydroxyimino)-carboxylic acids are specific and efficient coordinating ligands. Alternative donor centers of the oxime group (N,O_N) and the carboxylic group (O,O) lead to many different M−(2-hica) bindings: (1) monodentate through N or O atoms[13] and (2) bidentate through both carboxylic O, through O,N[1−10] or through O,O_N atoms, forming four-, five-, and six-membered stable rings, respectively. The O,N-bidentate complexes [M−(2-hica)$_2$] were found as cis[8] and trans isomers,[9] the first one being stabilized by hydrogen-bonding between a protonated and a deprotonated oxime group. The spontaneous deprotonation of the oxime group and stabilizing effect of the hydrogen-bond as well as the increasing oxime reactivity of the metal complexes prompt us to gain deeper insight into these processes with the help of first principles calculations.

Glyoxilic acid oxime (gao) is the simplest 2-(hydroxyimino)-carboxylic acid (HC(=NOH)COOH), and hence it is a suitable model to investigate its interaction with transition metal cations, both from an experimental and a theoretical point of view. The structure and vibrational properties of the gao monomer and tetramer were studied in detail.[19−21]

Although several theoretical studies have considered the alkaline, alkaline-earth,[22−28] and transition-metal cations (Ni^+, Cu^+, Cu^{2+}) binding to glycine,[23,24,26,29−38] to our knowledge no theoretical calculations have been performed for metal ions interacting with oxime analogues. In this paper we perform a theoretical study of the equilibrium geometries and binding energies of Cu^{2+} interacting with neutral glyoxilic acid oxime (gao) as well as with the anionic (gao^-) and dianionic (gao^{2-}) species derived from the deprotonation of the carboxylic and oxime groups. The electron distribution in neutral, anionic, and dianionic gao species presuppose different affinities of functional groups to Cu^{2+}; hence, different nature and strength of Cu^{2+}−gao, Cu^{2+}−gao^-, and Cu^{2+}−gao^{2-} bonding are anticipated.

The calculations have been done using different density functionals. A recent study on the ground and low-lying states of Cu^{2+}−H_2O has shown that the results can be quite sensitive to the amount of exact exchange included in the functional.[39] In addition, we have performed single-point calculations using the highly correlated CCSD(T) post-Hartree−Fock method. Results are compared with those previously obtained for Cu^{2+} interacting with glycine,[31] the parent amino acid of glyoxilic acid oxime.

II. Methods

Density functional methods have been widely used to study transition-metal-containing systems. However, recent studies on diverse Cu^{2+}−ligand systems carried out in our group have demonstrated that different functionals can provide different results when the degree of charge and spin delocalization of the system is important.[39] It was found that delocalized situations

* Corresponding authors. E-mail: mariona@klingon.uab.es (Sodupe); ntrend@svr.igic.bas.bg (Trendafilova).
† Institute of General and Inorganic Chemistry, Bulgarian Academy of Sciences.
‡ Universitat Autònoma de Barcelona.

are overstabilized by LDA and GGA functionals as a result of a bad cancellation of the self-interaction part by the exchange-correlation functional.[40] The admixture of exact exchange, which rigorously corrects for self-interaction, reduces the error. Because of that, the performance of different density functional methods has been analyzed for Cu^{2+}–gao.

Full geometry optimization and harmonic vibrational analysis for different isomers of Cu^{2+}–gao, Cu^{2+}–gao$^-$, and Cu^{2+}–gao^{2-} systems have been performed using the following functionals. For the correlation functional we have used the Lee, Yang, and Parr (LYP)[41] functional combined with the Becke's 1988 pure functional (B)[42] and two nonlocal hybrid exchange functionals, the Becke's three-parameter (B3),[43] and the Becke's half-and-half (BH)[44] functional. Furthermore, to confirm the density functional results, single-point coupled-cluster calculations with singles, doubles substitutions, and perturbational estimation of the triple excitations, CCSD(T),[45] have been performed at the B3LYP optimized geometries. A few calculations at the BHLYP optimized geometries have shown that the effect of the geometry on the relative CCSD(T) energies is small since results differ by less than 0.5 kcal/mol, regardless of whether we use B3LYP or BHLYP geometries. CCSD(T) calculations have been performed correlating all valence electrons.

Optimized structures are named as **n-**, **a-**, or **d-** to indicate if the interaction of Cu^{2+} takes place with neutral gao, with the anionic (gao$^-$), or the dianionic (gao^{2-}) species, respectively. The superscript (1 or 2) indicates whether the mode of binding is monodentate or bidentate, whereas the numbers in parentheses distinguish between conformers that share the same binding mode. For example, structure **n²-O,N(2)** is the second conformer found for Cu^{2+} interacting with neutral gao in a bidentate manner through the O and N atoms.

The following basis sets have been used. For Cu we employed the Watchers' primitive set (14s9p5d),[46] supplemented with one s, two p, and one d diffuse functions[46,47] and one f polarization function.[48] The final basis set is of the form (15s11p6d1f)/[10s7p4d1f]. For C, N, O, and H, the standard 6-31++G(d,p) basis set was employed. Hereafter, this basis set will be referred as Basis1. In some cases, single-point calculations have been performed with the enlarged 6-311++G(3df,2pd) basis set for C, N, O, and H atoms and the (15s11p6d2f1g)/ [10s7p4d2f1g] basis set for Cu^{2+} (Basis2).

All density functional calculations were performed using the Gaussian98 A.9 program package[49] and were based on an unrestricted formalism. The minima on the potential energy surfaces were qualified by the absence of negative eigenvalues in the diagonalized Hessian matrix, giving imaginary normal vibrational mode. The CCSD(T) results were obtained with the MOLPRO 2000.1 program[50] and were based on a spin-restricted formalism.

Electron spin densities on the atoms and net atomic charges have been obtained using the natural population analysis of Weinhold et al.[51]

III. Results and Discussion

Cu^{2+}–gao (neutral) Interaction. The conformational behavior of the neutral glyoxilic acid oxime has been studied in a recent theoretical study.[20] Among 16 conformations explored, four low-lying structures were located (see Scheme 1); the most stable one depends on the level of theory used.[20] Nevertheless, it should be noted that the relative energies of these conformers differ by less than 1 kcal/mol at the correlated (MP2 and

SCHEME 1

ectt   ecct   ettt   zccc
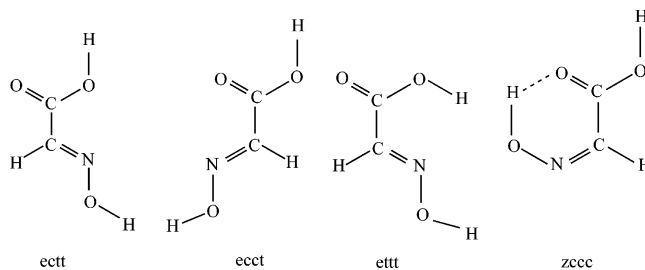
B3LYP) levels. The B3LYP/6-31++G(d,p) provides ectt as the lowest-energy conformer, in agreement with X-ray diffraction data.[19]

To analyze the binding properties of the ground state $^2D(d^9)$ of Cu^{2+} to glyoxilic acid oxime, we have considered as starting structures in the optimization process the attachment of Cu^{2+} to the electron-rich sites (O,N) of the low-lying conformers ectt, ecct, and ettt (see Scheme 1). The interaction of Cu^{2+} to the CO_2^- terminus of the zwitterionic form of gao has also been considered, since this was the most stable structure in the Cu^{2+}–glycine analogue. The coordination of Cu^{2+} to zccc was not considered because this conformer is stabilized by a strong intramolecular hydrogen bond, H···O and it is not suitable for coordination. In addition, the coordination of Cu^{2+} to other high-energy gao conformers, (etct, etcc, and zcct in ref 20) has been analyzed. Among all structures explored, only 12 were found as minima on the potential energy surface and they are shown in Figure 1.

It can be observed that six of the localized structures for Cu^{2+}–gao are monodentate: four with the carbonyl oxygen (O) binding site (gao is in different conformations) and two with the oxime oxygen (O_N) binding site, (see Figure 1). All monodentate structures, except **n¹-O$_N$(2)**, show C_1 symmetry, and the ground electronic state is ^2A. For **n¹-O$_N$(2)**, B3LYP and BHLYP provide C_s symmetry and a $^2A'$ ground electronic state, while with BLYP the C_s structure was found to be a first-order saddle point (58i cm^{-1}). In addition, six bidentate structures were found as stationary points: two with the metal cation coordinated to the CO_2^- group of zwitterionic gao, two with carbonylic O and N binding sites, one with carbonylic O and O_N binding sites, and one with hydroxylic oxygen (O_H) and oxime nitrogen (N) binding sites, see Figure 1. The **n²-O,N(1)** and **n²-O$_H$,N** conformers have C_1 symmetry and a ^2A ground state at all levels of theory, whereas the other four conformers, **n²-O,O(1)**, **n²-O,O(2)**, **n²-O,N(2)**, and **n²-O,O$_N$**, present C_s symmetry and a $^2A'$ ground state, except **n²-O,O$_N$** and **n²-O,N(2)** at the BLYP level which presents one imaginary frequency of about 200 cm^{-1}.

It is interesting to analyze the behavior of the different functionals upon determining the geometry parameters. In general, one can say that the different functionals tested provide similar geometry parameters, the most significant changes corresponding to the metal–ligand distances. However, the observed trends differ for monodentate and bidentate structures. For the first ones, the Cu^{2+}–ligand distances increase 0.13–0.22 Å upon increasing the amount of exact exchange in the functional (from BLYP to BHLYP), whereas for the bidentate structures, the Cu^{2+}–ligand distances decrease between 0.04 and 0.15 Å. The different trends obtained can be attributed to the different nature of the Cu^{2+}–gao interaction in the two kinds of coordination. For structures with monodentate coordination, natural population analysis indicates a significant charge transfer from glyoxilic acid oxime to Cu^{2+}, in such a way that the metal
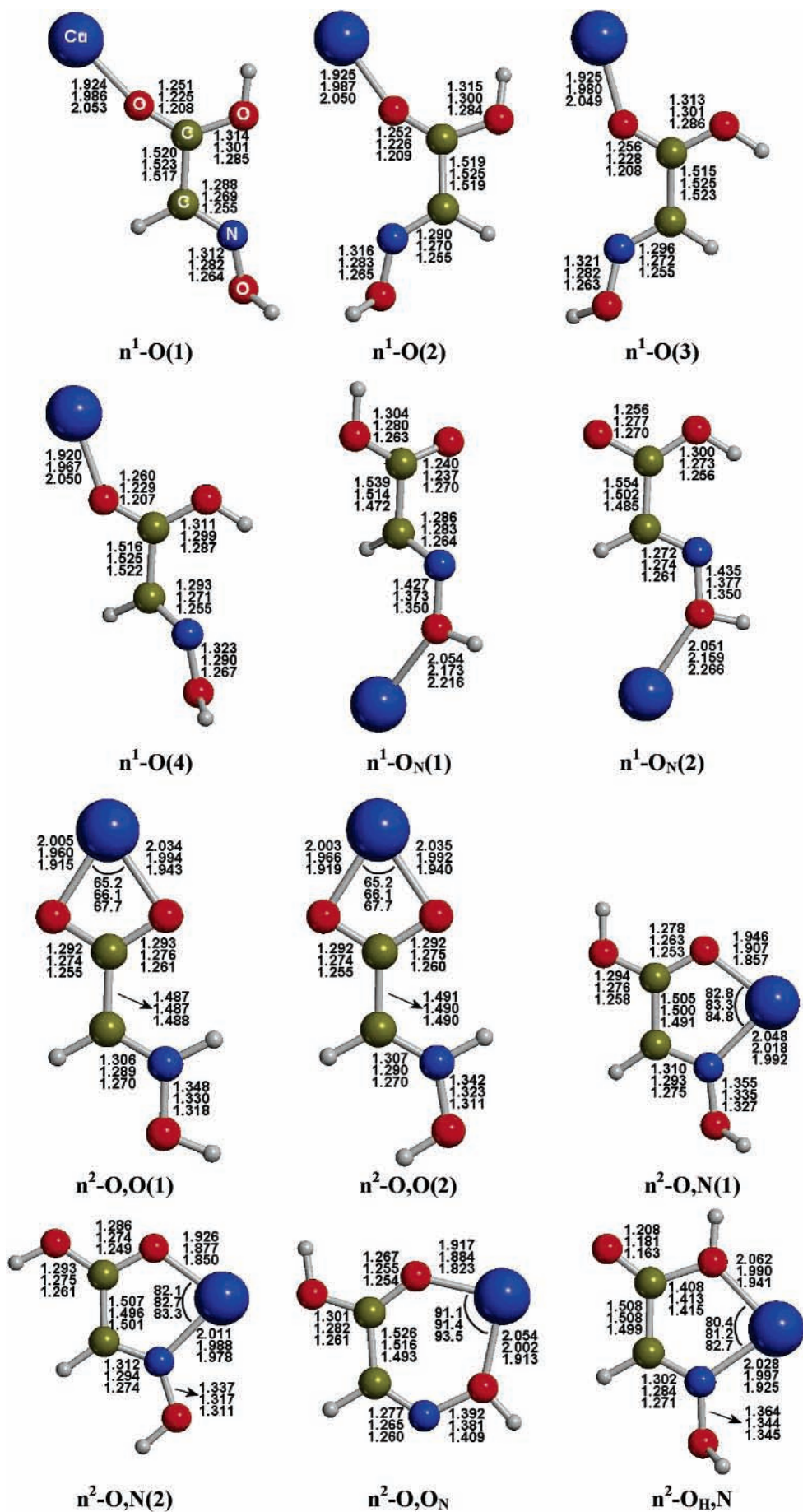
Figure 1. BLYP, B3LYP, and BHLYP optimized geometries for different minima of the Cu^{2+}−gao complex. Distances are in Å, and angles are in degrees.
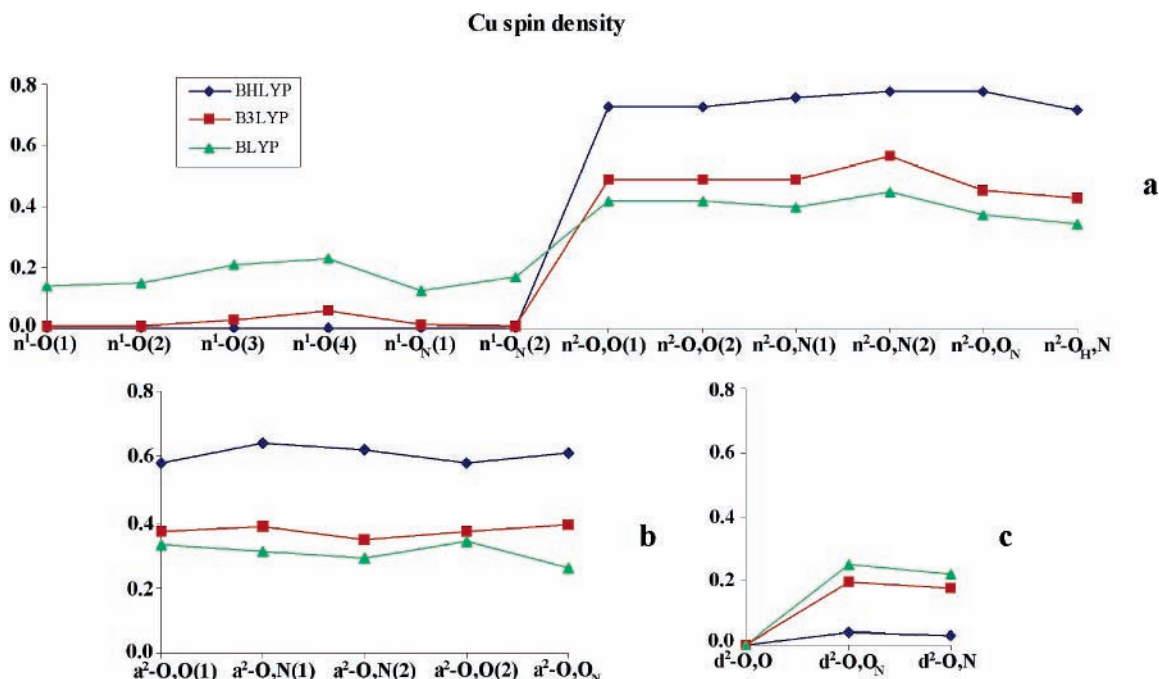
Figure 2. Spin density at Cu for (a) $Cu^{2+}-gao$, (b) $Cu^{2+}-gao^-$, and (c) $Cu^{2+}-gao^{2-}$.

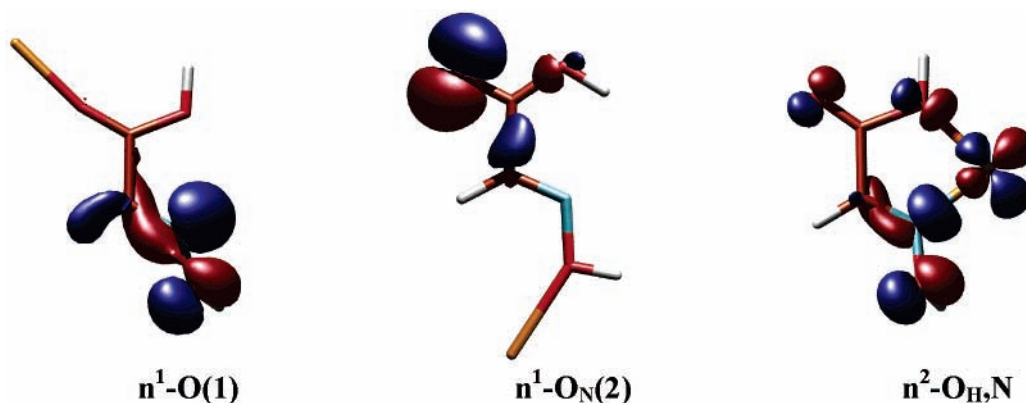**Figure 3.** Open shell orbital for different minima of the $Cu^{2+}-gao$ complex obtained at the B3LYP level.

ion behaves more as Cu^+ than as Cu^{2+}. Similar findings have been reported in the literature for guanine$^-$, uracil$^-$, and thiouracil$-Cu^{2+}$ complexes.[52,53] In these situations, the copper charge $q(Cu^{2+})$ is ~ 1, and the spin density at Cu^{2+} is small or close to 0 (see Figure 2). That is, the monodentate complexes appear to behave more as $Cu^+-gao^{\bullet+}$ than as $Cu^{2+}-gao$. Thus, variations on metal—ligand distances upon increasing the exact exchange respond to changes on electrostatic interactions and on the metal ability to reduce the repulsion by sd hybridization. It is observed that as the amount of exact exchange increases, sd hybridization becomes less effective and the metal—ligand distances increase.

In contrast, for bidentate complexes the spin density is more delocalized between the metal cation and gao. It can be observed in Figure 2, however, that the degree of delocalization depends on the functional used. At the BLYP level the spin density at the metal ion ranges from 0.35 to 0.45, whereas at the BHLYP level the spin density is 0.72—0.78 and copper behaves more as Cu^{2+} (d^9). It has been previously shown that delocalization between two fragments and with three electrons involved are overstabilized and present too large bond distances with LDA or GGA functionals. The overstabilization is due to a bad cancellation of the self-interaction (SI) included in the Coulomb energy by the exchange-correlation functional, the error increas-

ing with increasing distance (decreasing overlap between fragment orbitals).[39] Since the admixture of exact exchange reduces the error, the degree of delocalization and metal—ligand distances decrease the more the exchange functional is replaced by exact exchange.

The fact that the spin delocalization is larger in bidentate complexes than monodentate ones is related to the different metal 3d—gao orbital interactions upon changing the coordination environment. For bidentate coordinations the metal 3d orbital interacting with the N and O lone pairs of the ligand becomes significantly destabilized in such a way that this is the orbital that becomes monooccupied. However, for monodentate coordinations, the highest $3d\sigma$ orbital is less destabilized and the preferred situation corresponds to having the singly occupied orbital at gao. As an example, the open shell orbitals corresponding to two monodentate and one bidentate structures are shown in Figure 3. In agreement with the spin density distribution, the open shell orbital in the monodentate complexes is localized at the gao ligand. For $\mathbf{n^1-O(1)}$, the main contributions to the open shell orbital come from the p orbitals of N and O_N, and so spin density mainly lies at these atoms. For $\mathbf{n^1-O_N(2)}$, the open shell orbital has an important contribution of the p orbital of carbonyl O and the spin density mainly lies at this atom. In $\mathbf{n^2-O_H,N}$ the open shell orbital is delocalized

TABLE 1: Relative Energies (in kcal/mol) of Cu^{2+}−gao Isomers

			ΔE		
structure	BLYP	B3LYP	BHLYP	CCSD(T)[b]	ΔG^a
			monodentate		
n^1-O(1)	3.4	0.3	−3.6	−5.6	−8.3
n^1-O(2)	5.1	2.1	−1.7	−3.8	−6.5
n^1-O(3)	4.4	5.0	2.2	−0.3	−4.1
n^1-O(4)	3.3	4.5	2.4	0.2	−2.5
n^1-O$_N$(1)	27.1	26.6	19.5	21.2	17.4
n^1-O$_N$(2)	35.5	32.0	22.5	21.6	18.6
			bidentate		
n^2-O,O(1)	0.0	0.0	0.0	0.0	0.0
n^2-O,O(2)	1.9	2.2	2.2	2.1	2.4
n^2-O,N(1)	−1.1	−1.0	−2.8	2.3	2.9
n^2-O,N(2)	8.3	6.5	2.5	5.1	5.5
n^2-O,O$_N$	4.5	5.4	3.8	9.6	8.5
n^2-O$_H$,N	15.8	18.7	20.0	21.1	20.1

^{a} Obtained from RCCSD(T) energies and B3LYP thermal corrections at 298 K. ^{b} Single-point calculations at the B3LYP geometries.

all over the molecule, in agreement with the spin distribution. It can be observed that the metal 3d orbital polarizes away from the ligand by 3d−4p mixing in order to reduce the electron density along the metal−oxygen and metal−nitrogen directions, thereby reducing metal−ligand repulsion.

The computed relative energies using different density functionals as well as the highly correlated post-Hartree−Fock CCSD(T) method are given in Table 1. It can be observed that the relative energies are very sensitive to the functional used in such a way that with BLYP and B3LYP the ground-state structure is predicted to be bidentate **n^2-O,N(1)**, whereas with BHLYP and CCSD(T) the monodentate **n^1-O(1)** complex is the most stable one, the energy difference between the two structures ranging from 4.5 kcal/mol with BLYP to −7.9 kcal/mol with CCSD(T). Because the BSSE is larger for bidentate structures than for monodentate ones, **n^1-O(1)** becomes even more stable compared to bidentate structures when the counterpoise correction is included.[54] Thus, assuming the CCSD(T) energies as the reference values, it is observed that bidentate complexes are overstabilized with respect to monodentate ones with density functional methods, the degree of overstabilization decreasing the more the exchange functional is replaced by exact exchange. As mentioned above, for bidentate complexes, BLYP and also B3LYP, but to a lesser extent, provide a too delocalized picture of the electron hole (see Figure 2), a situation that is overstabilized by density functional methods as a result of a bad cancellation of self-interaction. While differences on relative energies are striking when comparing mono- and bidentate complexes, they become much less important within the same type of coordination. In particular, the B3LYP and BHLYP relative energies of monodentate complexes are in quite good agreement with CCSD(T) results. Thus, major differences appear when comparing situations with different spin distribution.

Among monodentate structures, all methods indicate that coordination to carbonylic oxygen is significantly preferred over coordination to oxime oxygen. On the other hand, it is interesting to note that the energy order of monodentate complexes does not follow the energy order of gao neutral conformers (ectt, ettt, ecct, and etct) but rather that of the corresponding gao radical conformers,[55] in agreement with the spin distribution found in these complexes. For bidentate complexes, the most stable structure at the CCSD(T) level corresponds to the coordination of Cu^{2+} to the CO$_2^-$ group of zwitterionic gao. However, coordination to N and to carbonylic O, **n^2-O,N(1)**, is somewhat more stable with all functionals and implies formation

TABLE 2: Interaction Energies (in kcal/mol) with Basis1 (Basis2)^a

structure	BLYP	B3LYP	BHLYP	CCSD(T)
Cu^{2+}−gao				
n^1-O(1)	230.6	211.9	188.5	191.5
	(230.6)	(212.3)	(189.1)	
n^2-O,O(1)	234.0	212.2	184.8	185.9
	(234.5)	(213.3)	(187.0)	
Cu^{2+}−glycine				
η^2-**O,O** (CO$_2^-$)	264.0	243.0	215.2	210.5
				(214.8)

^{a} Values for Cu^{2+}−glycine are taken from ref 31.

of a five-membered ring. Calculations suggest that upon Cu^{2+}− gao interaction, higher-energy conformers of gao give more stable bidentate complexes, **n^2-O,N(1)** and **n^2-O,N(2)**, than the one derived from the lowest gao conformer − **n^2-O$_H$,N**. More importantly, zwitterionic gao, which does not exist in the gas phase, becomes the most stable bidentate structure upon interaction with Cu^{2+}.

Interaction energies obtained with different functionals and at the CCSD(T) level are given in Table 2. For all complexes, the binding energy decreases upon augmenting the amount of exact exchange in the functional. These deviations from BLYP to BHLYP are larger for the bidentate structures (48−49 kcal/ mol) than for the monodentate ones (42 kcal/mol) because the spin density is more delocalized in the former species (see above). The main reason for this important variation in the Cu^{2+}−gao binding energy arises from the changes in the second ionization energy of Cu[56] at the different levels of calculation, which ranges from 21.2 eV at the BLYP/Basis1 level to 19.9 eV at the BHLYP/Basis1 level. That is, the Cu^{2+} + gao asymptote lies too high in energy with pure DFT functionals or with hybrid ones with a low percentage of exact exchange, and consequently the computed Cu^{2+}−gao binding energy is too large.

Glyoxilic Acid Oxime versus Glycine. Since glyoxilic acid oxime derives from glycine, a comparison of the ligand coordination behavior to Cu^{2+} is possible and informative. For glycine, the ground-state structure is derived from the interaction of Cu^{2+} with the CO$_2^-$ terminus of the zwitterionic form.[31] However, for Cu^{2+}−gao, this structure lies higher in energy than the O-monodentate ones because N$_{gao}$ has a lower basicity than N$_{glycine}$. For the same reason (and in contrast to Cu^{2+}− glycine), O-monodentate coordinations to carbonylic oxygen are more stable than O,N bidentate ones. Note that whereas Cu^{2+}− O(monodentate) distances are similar in glycine and glyoxilic acid oxime complexes, the Cu^{2+}−O,N(bidentate) distances are smaller in Cu^{2+}−glycine.[31] As a consequence of these coordination differences, the interaction energies of Cu^{2+}−glycine and Cu^{2+}−gao also show significant differences (see Table 2). At all levels of calculation, the interaction energy of Cu^{2+} to glycine (assuming the η^2-**O,O(CO$_2^-$)** ground-state complex) is about 20−35 kcal/mol larger than the interaction energy of Cu^{2+} to gao (**n^1-O(1)**).

Cu^{2+}−gao$^-$ (anion) Interaction. Both deprotonation energies and pK_a values suggest that first deprotonation of glyoxilic acid oxime occurs at the carboxylic group. Thus, only deprotonation of the COOH group was considered. The conformational study of the gao$^-$ provided four different low-lying structures (Scheme 2).[20]

As in the case of Cu^{2+}−gao, the complexes derived from the coordination of Cu^{2+} to the oxygen and nitrogen atoms of these low-lying conformers were considered as starting structures in the optimization procedure (the z1$^-$ conformer was not
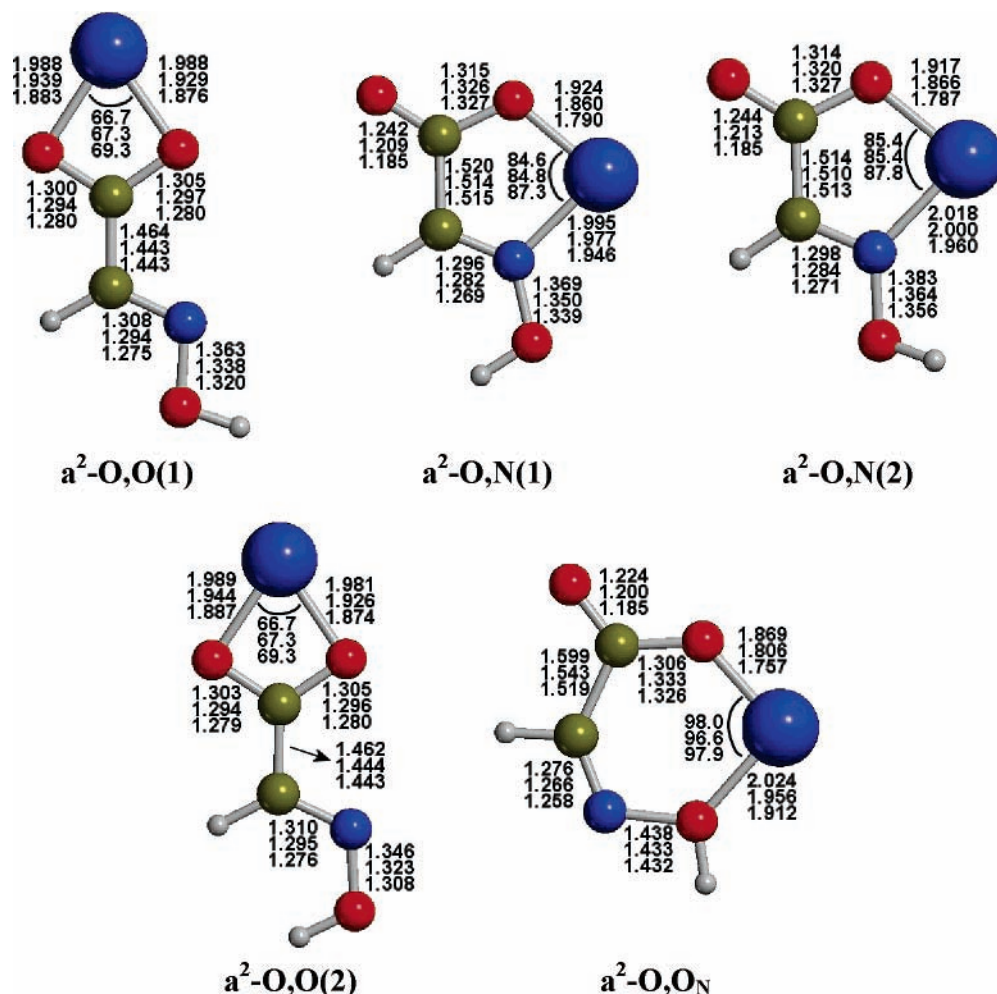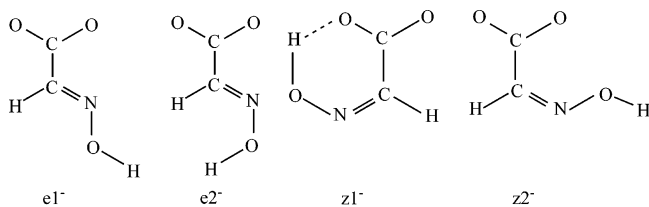
Coordination of Oxime Analogue of Glycine to Cu(II)

J. Phys. Chem. A, Vol. 109, No. 25, 2005 **5673**

Figure 4. BLYP, B3LYP, and BHLYP optimized geometries for different minima of the Cu^{2+}−gao$^-$ complex. Distances are in Å, and angles are in degrees.

SCHEME 2

considered since it is unsuitable for a coordination). Figure 4 shows the five structures found as minima on the potential energy surface. All of them are bidentate: two coordinated O,N, two O,O, and one O,O$_N$, forming five-, four-, and six-membered rings, respectively. In all cases, except the **a²-O,N(2)** one, the optimized B3LYP and BHLYP structures have C_s symmetry and the lowest electronic state is $^2A'$. The deviation of **a²-O,N-(2)** structure from C_s symmetry is, however, small (0.08 kcal/mol at the B3LYP level) and concerns only the hydrogen oxime atom. On the other hand, C_s structures for **a²-O,O(1)**, **a²-O,O-(2)**, and **a²-O,O$_N$** are first-order saddle points at the BLYP level.

It can be observed in Figure 4 that, in general, the metal−ligand distances are somewhat smaller for the Cu^{2+}−gao$^-$ isomers than for the Cu^{2+}−gao ones as a result of the enhancement of the electrostatic interaction between Cu^{2+} and deprotonated glyoxilic acid oxime (gao$^-$). On the other hand, the geometrical parameters obtained at different levels of theory follow the same trends mentioned above for the bidentate Cu^{2+}−gao complexes. That is, the most important differences between

functionals correspond to the metal−ligand distances, which decrease upon increasing the amount of exact exchange in the functional, especially that of Cu^{2+}−O, which decreases about 0.11−0.13 Å. As in Cu^{2+}−gao, the spin density is partially delocalized between the metal cation and the ligand, the degree of delocalization depending on the functional. The main difference is that the spin density over the metal atom is somewhat smaller for the Cu^{2+}−gao$^-$ structures than for the analogous Cu^{2+}−gao bidentate ones with all the considered functionals (see Figure 2) due to the different total charge of the complex, which makes the L → Cu^{2+} charge transfer more efficient.

Figure 5 shows two examples of open shell orbitals of Cu^{2+}−gao$^-$. As for Cu^{2+}−gao, the open shell orbitals in bidentate situations are delocalized between the metal atom and the ligand, in agreement with the spin distribution, and the metal 3d orbital polarizes in order to reduce the metal−ligand repulsion.

The relative energies of the different structures computed with every method are shown in Table 3. In this case different functionals provide results in reasonable agreement with the CCSD(T) values. It should be remembered that for Cu^{2+}−gao$^-$ the coordination is always bidentate, and the description of the electron hole is similar for all the structures. Consequently, we are comparing situations with a similar spin distribution.

The most stable structure predicted by all methods is **a²-O,O-(1)**. Such a O,O bidentate structure was found as the most stable in Cu^{2+}−glycine (zwitterionic) interaction.[31] Next in energy are **a²-O,N(1)** and **a²-O,N(2)** structures which are about 2 kcal/
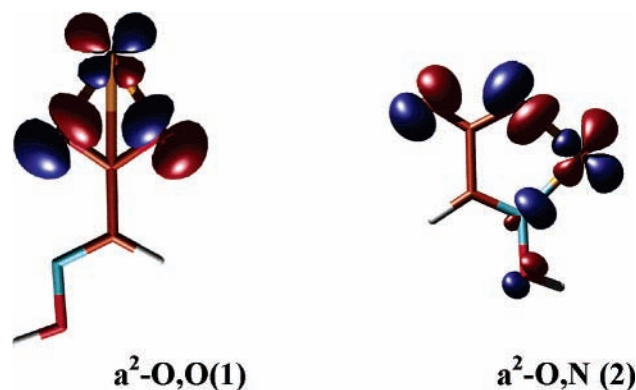
Figure 5. Open shell orbital for different minima of the Cu^{2+}−gao$^-$ complex obtained at the B3LYP level.

**TABLE 3: Relative Energies (in kcal/mol) of Cu^{2+}−gao$^-$ Isomers**

		ΔE			
structure	BLYP	B3LYP	BHLYP	CCSD(T)^b	ΔG^a
a^2-O,O(1)	0.0	0.0	0.0	0.0	0.0
a^2-O,N(1)	1.7	4.2	2.8	1.9	1.7
a^2-O,N(2)	0.8	4.0	3.8	2.1	1.5
a^2-O,O(2)	7.7	7.7	7.8	8.0	7.7
a^2-O,O$_N$	8.7	11.8	11.2	8.3	6.3

^{a} Obtained from RCCSD(T) energies and B3LYP thermal corrections at 298 K. ^{b} Single-point calculations at the B3LYP geometries.

mol above the global minimum at the CCSD(T) level. They have O,N-binding and differ only by the orientation of the oxime H atom. The **a^2-O,O(2)** structure lies 8 kcal/mol above the most stable structure and differs from it by the orientation of the oxime hydrogen atom. A survey of the results for the bidentate Cu^{2+}−gao$^-$ structures shows that the conformation of gao$^-$ in the higher-energy structure **a^2-O,O(2)** is that corresponding to the highest-energy conformer of the free anion, e2$^-$, (3 kcal/mol above the e1$^-$ conformer), whereas the low-energy **a^2-O,O-(1)** structure contains the most stable anion conformer, e1$^-$, which arises from the lowest neutral ectt conformer.[20] The **a^2-O,O$_N$** is the highest-energy structure with 8.3 kcal/mol above the **a^2-O,O(1)** structure.

As expected, carboxylic oxygen atoms of the gao anion are more basic than the N atom.[20] In fact, we did not succeed in obtaining the N gas-phase basicity, since spontaneous proton transfer from N to O atom (in the cis position) occurred. This

SCHEME 3
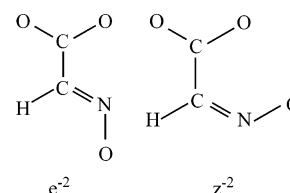
result would suggest entirely a weaker gas-phase basicity of N, compared to those of carboxylic O atoms, in agreement with the largest stability of the **a^2-O,O(1)** structure, given that the electrostatic interaction is the main force in Cu^{2+}−gao$^-$ complexes.

The theoretical study of Cu^{2+}−gao$^-$ interaction is informative with a view of the further investigation of this interaction in aqueous solution, since a comparison with experiment is possible. Usually, the coordination complexes found in aqueous solution are confirmed by X-ray diffraction analysis. X-ray data have shown that the methyl derivative of a gao anion coordinates to Cu^{2+} in a bidentate manner through N oxime and carboxylic O atoms.[3,8] This is in contrast to our gas-phase results which provide **a^2-O,O(1)** as the most stable structure, the **a^2-O,N** ones lying only 2 kcal/mol above. Although in all cases the interaction is mainly of electrostatic nature, other factors also contribute to the interaction. It is possible that upon solvation in aqueous solution, other energy contributions become important for **a^2-O,O(1)** and **a^2-O,N** stabilization. Since the energy difference between these two isomers is small, its relative energy order could reverse.

Cu^{2+}−gao^{2-} (dianion) Interaction. Figure 6 shows the three structures found as minima upon the interaction of Cu^{2+} with the two conformers of gao^{2-} (Scheme 3). All of the localized structures are bidentate and have C_s symmetry at all levels of theory, the lowest electronic state being ^{2}A′. The structures found correspond to the coordination of the metal cation to one carboxylic O and the oxime oxygen (**d^2-O,O$_N$**), to one carboxylic O and N (**d^2-O,N**), and to both carboxylic oxygens (**d^2-O,O**).

It is interesting to note that for Cu^{2+}−gao^{2-} the behavior of the metal−ligand distances is not the same for all structures and differs from that observed in Cu^{2+}−gao and Cu^{2+}−gao$^-$ bidentate complexes. For the **d^2-O,O** conformer, the metal−oxygen distances decrease from BLYP to BHLYP, but the observed decrease (∼0.01 Å) is much smaller than in previous
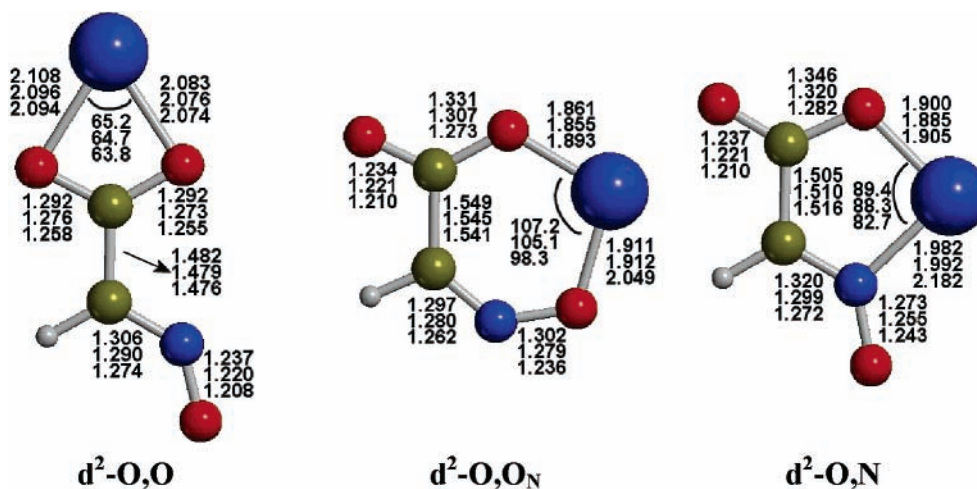

Figure 6. BLYP, B3LYP, and BHLYP optimized geometries for different minima of the Cu^{2+}−gao^{2-} complex. Distances are in Å, and angles are in degrees.
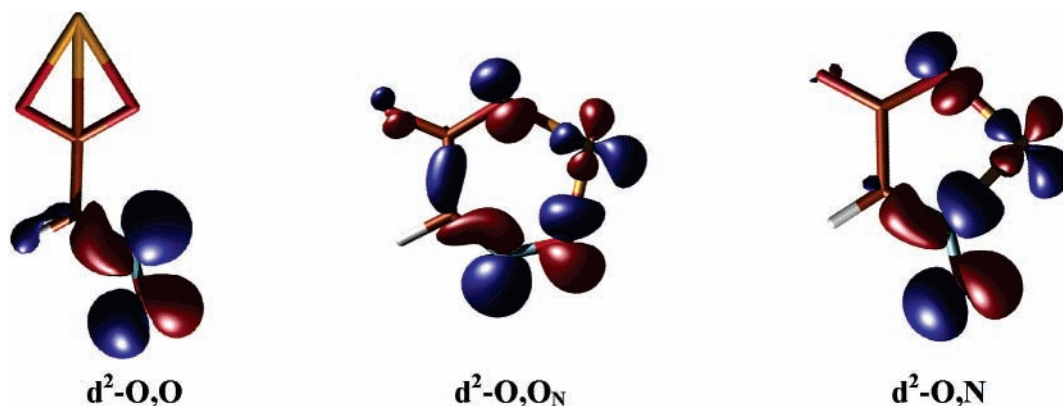
Figure 7. Open shell orbital of different minima of the $Cu^{2+}-gao^{2-}$ complex obtained at the B3LYP level.

TABLE 4: Relative Energies (in kcal/mol) of $Cu^{2+}-gao^{2-}$ Isomers

structure	ΔE				ΔG^a
	BLYP	B3LYP	BHLYP	$CCSD(T)^b$	
d^2-O,O	0.0	0.0	0.0	0.0	0.0
d^2-O,O_N	−11.4	−4.4	3.0	2.3	3.0
d^2-O,N	−6.4	1.2	7.8	7.4	8.3

^{a} Obtained from RCCSD(T) energies and B3LYP thermal corrections at 298 K. ^{b} Single-point calculations at the B3LYP geometries.

systems ($\sim$0.1 Å). For the other two structures, the Cu−O distances slightly increase, whereas the Cu−N distances increase significantly (0.14 and 0.2 Å). For $Cu^{2+}-gao^{2-}$ structures, the computed metal charge is always between 0.8 and 1.0, indicating an important charge transfer from the ligand to the metal atom and the spin density is more localized at the ligand, especially for **d^2-O,O**, for which all methods provide spin zero at the metal ion. A larger charge transfer compared to bidentate $Cu^{2+}-gao$ or $Cu^{2+}-gao^-$ complexes is not surprising considering that now Cu^{2+} is interacting with a dianion. As in the previous systems, for **d^2-O,O_N** and **d^2-O,N** the spin density becomes more localized as the amount of exact exchange included in the functional increases. The main difference is that the increase of the spin density is produced at the ligand and not at the metal cation. For these complexes with very large electrostatic interactions and small delocalization, the main geometry variations from BLYP and BHLYP are not dominated by the effects of self-interaction error. Changes are more complex, variations on the electron density of the ligand being probably the main factor. Open shell orbitals for the dianion complexes are shown in Figure 7.

Table 4 shows the relative energies of the three structures at different levels of theory. It can be observed that the computed relative energies between **d^2-O,O_N** and **d^2-O,N** are very similar with all functionals, the **d^2-O,O_N** conformer being about 5 kcal/mol more stable than **d^2-O,N**. However, the situation completely changes when these structures are compared with **d^2-O,O**. The energy difference between **d^2-O,O** and **d^2-O,O_N** varies from 11.4 at the BLYP level to −2.3 kcal/mol at the CCSD(T) level, showing that **d^2-O,O_N** (and also **d^2-O,N**) are overstabilized with respect to **d^2-O,O** by density functional methods. Again, this can be attributed to the larger spin delocalization in **d^2-O,O_N** and **d^2-O,N** with BLYP and B3LYP functionals (see Figure 2).

The **d^2-O,O** most stable structure and **d^2-O,N** contain the dianion in the lowest-energy conformer, e^{2-}. Hence, in the gas phase the most probable structure is **d^2-O,O**. Solvent effects may, however, reverse the relative energy order of the structures studied.[57,58]

IV. Conclusions

The coordination properties of glyoxilic acid oxime (gao)—the oxime analogue of glycine amino acid—and its deprotonated (gao$^-$ and gao^{2-}) species to Cu^{2+} have been studied with different density functional methods and CCSD(T) post-Hartree−Fock method. The isomers studied involve coordination of Cu^{2+} to electron-rich sites (O,N) of neutral, anionic, and dianionic gao species in different conformation.

Calculations suggest a different global minimum structure for Cu^{2+} interacting with glyoxilic acid oxime rather than with glycine. For Cu^{2+}−glycine, the ground-state structure is bidentate and derives from the interaction of Cu^{2+} with the CO_2^- terminus of zwitterionic glycine. However, for Cu^{2+}−gao such a zwitterionic structure lies higher in energy, and the most stable isomer shows monodentate binding of Cu^{2+} with the carbonylic oxygen, **n^1-O(1)**. Differences can be attributed to the decrease of N basicity in the oxime analogue. The computed Cu^{2+}−gao interaction energy (192 kcal/mol) is smaller than that of Cu^{2+}−glycine (211 kcal/mol). Deprotonated gao species (gao$^-$ and gao^{2-}) also prefer interaction with carboxylic oxygens but in a bidentate manner (**a^2-O,O(1)** and **d^2-O,O**, respectively).

Monodentate coordinations with neutral gao show an important gao → Cu^{2+} charge transfer in such a way that they behave more as Cu^+−gao$^{\bullet+}$ than as Cu^{2+}−gao. In bidentate coordinations, the spin density is more delocalized between the metal cation and the ligand. For these open shell (Cu^{2+}−L) systems, the relative stability of complexes with different coordination environments (and thus different spin distribution) can be quite sensitive to the amount of Hartree−Fock exchange included in the functional. Among all the functionals tested in this work, the BHandHLYP is the one that better compares to CCSD(T) results.

References and Notes

(1) Onindo, Ch. O.; Sliva, T. Yu.; Kowalik-Jankowska, T.; Fritsky, I. O.; Buglyo, P.; Pettit, L. D.; Kozlowski, H.; Kiss, T. *J. Chem. Soc.*, *Dalton Trans.* **1995**, 3911.

(2) Sliva, T. Yu.; Kowalik-Jankowska, T.; Amirkhanov, V. M.; Glowiak, T.; Onindo, Ch. O.; Fritsky, I. O.; Kozlowski, H. *J. Inorg. Biochem.* **1997**, *65*, 287.

(3) Sliva, T. Yu.; Dobosz, A.; Jerzykiewicz, L.; Karaczyn, A.; Moreeuw, A. M.; Swiatek-Kozlowska, J.; Glowiak, T.; Kozlowski, H. *J. Chem. Soc.*, *Dalton Trans.* **1998**, 1863.

(4) Mokhir, A. A.; Gumienna-Kontecka, E.; Swiatek-Kozlowska, J.; Petkova, E.; Fritsky, I. O.; Jerzykiewicz, L.; Kapshuk, A.; Sliva, T. Yu. *Inorg. Chim. Acta* **2002**, *329*, 113.

(5) Skopenko, V. V.; Lampeka, R. D.; Sliva, T. Yu.; Sakhov, D. I. *Ukr. Khim. Zh.* (*Russ. Ed.*) **1990**, *56* (7), 675.

(6) Sliva, T. Yu.; Lampeka, R. D.; Usakbergenova, Z. D.; Amirkhanov, V. M.; Jumabaev, A. J. *Ukr. Khim.* Zh. (*Russ. Ed.*) **1991**, *57* (9), 904.

(7) Trendafilova, N.; Bauer, G.; Georgieva, I.; Dodoff, N. *Spectrochim. Acta A* **1999**, *55*, 2849.

(8) Simonov, Yu. A.; Sliva, T. Yu.; Mazus, M. D.; Dvorkin, A. A.; Lampeka, R. D. *Zh. Neorg. Khim.* (*Russ. Ed.*) **1989**, *34* (4), 873.

(9) Lampeka, R. D.; Dudarenko, N. M.; Skopenko, V. V. *Acta Crystallogr. C50* **1994**, 706.

(10) Dvorkin, A. A.; Simonov, Yu. A.; Sliva, T. Yu.; Lampeka, R. D.; Mazus, M. D.; Skopenko, V. V.; Malinovskii, T. I. *Zh. Neorg. Khim.* (*Russ. Ed.*) **1989**, *34* (10), 2582.

(11) Skopenko, V. V.; Sliva, T. Yu.; Simonov, Yu. A.; Dvorkin, A. A.; Mazus, M. D.; Lampeka, R. D.; Malinovskii, T. I. *Zh. Neorg. Khim.* (*Russ. Ed.*) **1990**, *35* (7), 1743.

(12) Lampeka, R. D.; Skopenko, V. V.; Sliva, T. Y.; Khenning, K. *Ukr. Khim. Zh.* (*Russ. Ed.*) **1988**, *54*, 675.

(13) Apblett, A. W.; Georgieva, G. D.; Mague, J. T. *Inorg. Chem.* **1997**, *36*, 2656.

(14) Keeney, M. E.; Osseo-Asare, K.; Wood, K. A. *Coord. Chem. Rev.* **1984**, *59*, 141 and references therein.

(15) Apblett, A. W.; Lei, J.; Georgieva, G. D. In *Better Ceramics Through Chemistry V.*; *Mater. Res. Soc.* Symp. Proc., Vol. 271; Hampden-Smith, M. J., Klemperer, W. G., Brinker, C. J., Eds.; Materials Research Society: Pittsburgh, PA, 1992; pp 77−82. (b) Apblett, A. W.; Georgieva, G. D. *Phosphorus, Sulfur Silicon Relat. Elem.* **1994**, 93.

(16) Kukushkin, V. Yu.; Tudela, D.; Pombiero, A. J. L. *Coord. Chem. Rev.* **1996**, *156*, 333.

(17) Ruiz, R.; Sanz, J.; Cervera, B.; Lloret, F.; Julve, M.; Bois, C.; Faus, J.; Munoz, M. C. *J. Chem. Soc.*, Dalton Trans. **1993**, 1623.

(18) Mansuy, D.; Battioni, P.; Battioni, J.-P. *Eur. J. Biochem.* **1989**, *184*, 267. (b) Meunier, B. *Chem.* Rev. **1992**, *92*, 1411. (c) Custot, J.; Boucher, J.-L.; Vadov, S.; Guedes, C.; Dijols, S.; Delaforge, M.; Mansuy, D. *J. Biol. Inorg. Chem.* **1995**, *1*, 73.

(19) Georgieva, I.; Binev, D.; Trendafilova, N.; Bauer, G. *Chem. Phys.* **2003**, *286*, 205.

(20) Trendafilova, N.; Bauer, G.; Georgieva, I.; Delchev, V. *J. Mol. Struct.* **2002**, *604*, 211.

(21) Georgieva, I.; Trendafilova, N.; Binev, D. *Vib. Spectrosc.* **2003**, *31*, 143.

(22) Hoyau, S.; Ohanessian, G. *Chem. Eur. J.* **1998**, *4*, 1561.

(23) Marino, T.; Russo, N.; Toscano N. *J. Inorg. Biochem.* **2000**, *79*, 179.

(24) Pulkkinen, S.; Noguera, M.; Rodríguez-Santiago, L.; Sodupe, M.; Bertrán, J. *Chem. Eur. J.* **2000**, *6*, 4393.

(25) Strittmatter, E. F.; Lemoff, A. S.; Williams, E. R. *J. Phys. Chem. A* **2000**, *104*, 9793.

(26) Hoyau, S.; Pélicier, J.-P.; Rogalewicz, F.; Hoppilliard, Y.; Ohanessian, G. *Eur. J. Mass Spectrom.* **2001**, *7*, 303.

(27) Moision, R. M.; Armentrout, P. B. *J. Phys. Chem. A* **2002**, *106*, 10350.

(28) Wong, C. H. S.; Siu, F. M.; Ma, N. L.; Tsang, C. W. *J. Mol. Struct.* (*THEOCHEM*) **2002**, *588*, 9.

(29) Hoyau, S.; Ohanessian, G. *J. Am. Chem. Soc.* **1997**, *119*, 2016.

(30) Bruin, T. J. M.; Marcelis, A. T. M.; Zuilhof, H.; Sudhölter, E. J. R. *Phys. Chem. Chem. Phys.* **1999**, *1*, 4157.

(31) Bertran, J.; Rodriguez-Santiago, L.; Sodupe, M. *J. Phys. Chem. B* **1999**, *103*, 2310.

(32) Hoppilliard, Y.; Ohanessian, G.; Bourcier, S. *J. Phys. Chem. A* **2004**, in press.

(33) Rogalewicz, F.; Ohanessian, G.; Gresh, N. *J. Comput. Chem.* **2000**, *21*, 963.

(34) Rodriguez-Santiago, L.; Sodupe, M.; Tortajada, J. *J. Phys. Chem. A* **2001**, *105*, 5340. (b) Constantino, E.; Rodríguez-Santiago, L.; Sodupe, M.; Tortajada, J. *J. Phys. Chem. A* **2005**, *109*, 224.

(35) Shoeib, T.; Siu, K. W. M.; Hopkinson, A. C. *J. Phys. Chem. A* **2002**, *106*, 6121.

(36) Ai, H.; Bu, Y.; Han, K. *J. Chem. Phys.* **2003**, *118*, 10973.

(37) Lemoff, A. S.; Bush, M. F.; Williams, E. R. *J. Am. Chem. Soc.* **2003**, *125*, 13576.

(38) Rogalewicz, F.; Hoppilliard, Y.; Ohanessian, G. *Int. J. Mass Spectrom.* **2003**, *227*, 439.

(39) Poater, J.; Sola, M.; Rimola, A.; Rodriguez-Santiago, L.; Sodupe, M. *J. Phys. Chem. A* **2004**, *108*, 6072.

(40) Sodupe, M.; Bertran, J.; Rodriguez-Santiago, L.; Baerends, E. J. *J. Phys. Chem. A* **1999**, *103*, 166.

(41) Lee, C.; Yang, W.; Parr, R. G. *Phys. Rev. B* **1988**, *37*, 785.

(42) Becke, A. D. *Phys. Rev. A* **1988**, *38*, 3098.

(43) Becke, A. D. *J. Chem. Phys.* **1993**, *98*, 5648.

(44) Becke, A. D. *J. Chem. Phys.* **1993**, *98*, 1372.

(45) Raghavachari, K.; Trucks, G. W.; Pople, J. A.; Head-Gordon, M. *Chem. Phys. Lett.* **1989**, *57*, 479.

(46) Watchers, A. J. H. *J. Chem. Phys.* **1970**, *52*, 1033.

(47) Hay, P. J. *J. Chem. Phys.* **1977**, *66*, 4377.

(48) Raghavachari, K.; Trucks, G. W. *J. Chem. Phys.* **1989**, *91*, 1062.

(49) Frisch, M. J.; Trucks, G. W.; Schlegel, H. B.; Scuseria, G. E.; Robb, M. A.; Cheeseman, J. R.; Zakrzewski, V. G.; Montgomery, J. A., Jr.; Stratmann, R. E.; Burant, J. C.; Dapprich, S.; Millam, J. M.; Daniels, A. D.; Kudin, K. N.; Strain, M. C.; Farkas, O.; Tomasi, J.; Barone, V.; Cossi, M.; Cammi, R.; Mennucci, B.; Pomelli, C.; Adamo, C.; Clifford, S.; Ochterski, J.; Petersson, G. A.; Ayala, P. Y.; Cui, Q.; Morokuma, K.; Malick, D. K.; Rabuck, A. D.; Raghavachari, K.; Foresman, J. B.; Cioslowski, J.; Ortiz, J. V.; Baboul, A. G.; Stefanov, B. B.; Liu, G.; Liashenko, A.; Piskorz, P.; Komaromi, I.; Gomperts, R.; Martin, R. L.; Fox, D. J.; Keith, T.; Al-Laham, M. A.; Peng, C. Y.; Nanayakkara, A.; Gonzalez, C.; Challacombe, M.; Gill, P. M. W.; Johnson, B.; Chen, W.; Wong, M. W.; Andres, J. L.; Gonzalez, C.; Head-Gordon, M.; Replogle, E. S.; Pople, J. A. *Gaussian 98*, *Revision A.9*; Gaussian, Inc.: Pittsburgh, PA, 1998.

(50) MOLPRO is a package of ab initio programs written by H. J. Werner and P. J. Knowles, with contributions from Almlöf, J.; Amos, R. D.; Berning, A.; Cooper, D. L.; Deegan, M. J. O.; Dobbyn, A. J.; Eckert, F.; Elbert, S. T.; Hampel, C.; Lindh, R.; Lloyd, W.; Meyer, W.; Nicklass, A.; Peterson, K.; Pitzer, R.; Stone, A. J.; Taylor, P. R.; Mura, M. E.; Pulay, P.; Schütz, M.; Stoll, H.; Thorsteinsson, T. The RCCSD program is described in the following: Knowles, P. J.; Hampel, C.; Werner, H.-J. *J. Chem. Phys.* **1993**, *99*, 5219.

(51) Reed, A. E.; Curtiss, L. A.; Weinhold, F. *Chem. Rev.* **1988**, *88*, 899.

(52) Lamsabhi, A. M.; Alcamí, M. T. Mo, O.; Yánez, M.; Tortajada, J. *ChemPhysChem* **2004**, *5*, 1871.

(53) Noguera, M.; Bertran, J.; Sodupe, M. *J. Phys. Chem. A* **2004**, *108*, 333.

(54) The computed counterpoise corrections, at the CCSD(T) level, for **n¹-O(1)** and **n²-O,O(1)** are 2.0 and 4.6, respectively.

(55) The relative order of gao conformers calculated at B3LYP/6-31++G(d,p) level is as follows: ectt (0.0 kcal/mol) < ettt (0.59 kcal/mol) < ecct (0.76 kcal/mol) < etct (7.63 kcal/mol). The relative order of radical cation conformers is as follows: ectt•⁺ (0.0 kcal/mol) < ecct•⁺ (0.05 kcal/mol) < ettt•⁺ (5.26 kcal/mol) < etct•⁺ (5.26 kcal/mol).

(56) The experimental value lies between the B3LYP and BHLYP ones (20.3 eV). NIST, *http://www.nist.gov*.

(57) Arnet, E. M. *Acc. Chem. Res.* **1973**, *6*, 404.

(58) Aue, D. H.; Webb, H. M.; Bowers, M. T. *J. Am. Chem. Soc.* **1976**, *21*, 318.